Contrib Mineral Petrol (1987) 96:24–34

Contributions to Mineralogy and Petrology

The kinetics of nucleation and crystal growth and scaling laws for magmatic crystallization

Genevieve Brandeis and Claude Jaupart
Institut de Physique du Globe, Université Paris 6 et 7, 4 place Jussieu, F-75252 Paris Cédex 05, France

Abstract. Magmatic crystallization depends on the kinetics of nucleation and crystal growth. It occurs over a region of finite thickness called the crystallization interval, which moves into uncrystallized magma. We present a dimensional analysis which allows a simple understanding of the crystallization characteristics. We use scales for the rates of nucleation and crystal growth, denoted by I_m and Y_m respectively. The crystallization time-scale τ_c and length-scale d_c are given by $(Y_m^3 \cdot I_m)^{-1/4}$ and $(\kappa \cdot \tau_c)^{1/2}$ respectively, where κ is thermal diffusivity. The thickness of the crystallization interval is proportional to this length-scale. The scale for crystal sizes is given by $(Y_m/I_m)^{1/4}$. We use numerical calculations to derive dimensionless relationships between all the parameters of interest: position of the crystallization front versus time, thickness of the crystallization interval versus time, crystal size versus distance to the margin, temperature versus time. We assess the sensitivity of the results to the form of the kinetic functions. The form of the growth function has little influence on the crystallization behaviour, contrary to that of the nucleation function. This shows that nucleation is the critical process. In natural cases, magmatic crystallization proceeds in continously evolving conditions. Local scaling laws apply, with time and size given by $\tau = (Y^3 \cdot I)^{-1/4}$ and $R = (Y/I)^{1/4}$, where Y and I are the rates at which crystal are grown and nucleated locally. τ is the time to achieve crystallization and R the mean crystal size. We use these laws together with petrological observations to infer the in-situ values of the rates of nucleation and growth. Two crystallization regimes are defined. In the highly transient conditions prevailing at the margins of basaltic intrusions, undercoolings are high and the peak nucleation and growth rates must be close to $1\ \mathrm{cm}^{-3} \cdot \mathrm{s}^{-1}$ and 10^{-7} cm/s, in good agreement with laboratory measurements. In quasi-equilibrium conditions prevailing in the interior of large intrusions, undercoolings are small. We find ranges of 10^{-7} to $10^{-3}\ \mathrm{cm}^{-3}\ \mathrm{s}^{-1}$ and of 10^{-10} to 10^{-8} cm/s for the local rates of nucleation and growth respectively.

I Introduction

In a magma chamber, crystallization is affected by many processes. Igneous layering and crystal size variations show that crystallization does not proceed continuously, with the thickness of the crystal pile increasing at a steady rate. To interpret this complex igneous record, one must first understand the very process of crystallization. For natural magmas, it occurs out of equilibrium and depends on the kinetics of nucleation and crystal growth. Following an early attempt by Kirkpatrick (1976), Brandeis et al. (1984) studied the transient cooling of magma emplaced in cold country rocks. Given functions for the rates of nucleation and crystal growth, the evolution of crystallization can be followed and all relevant parameters can be computed. These include the thickness of the crystallization interval, which is the region where crystallization is active, and the crystal size. The calculations are made with a computer program which has two drawbacks: they do not allow a straightforward understanding of the characteristics of crystallization and must be repeated for each new system studied. The latter is particularly limiting since there are few data on the rates of nucleation and growth. The purpose of this paper is to present a dimensional analysis of the same problem. Given scales for the rates of nucleation and crystal growth, we derive a time-scale for crystallization, a length-scale (proportional to the thickness of the crystallization interval) and finally a size-scale (proportional to the crystal size). This leads to a very simple method to characterize crystallization.

Before proceeding with the analysis, a few words may be useful to explain why such a general understanding of crystallization equations is needed. The past ten years have seen many dynamic crystallization experiments in the laboratory (Gibb 1974; Walker et al. 1976; Donaldson 1979; Lofgren 1980; Kirkpatrick et al. 1981; Tsuchiyama 1983; Baker and Grove 1985). To use them for petrological interpretations, it is necessary to estimate the cooling rate in natural conditions. This is usually done with the simple thermal calculations of Jaeger (1968), which is not legitimate because the crystallization kinetics have an effect on the cooling rate through the release of latent heat (Dowty 1980; Brandeis et al. 1984). Therefore, the full problem must be solved, which requires the knowledge of the nucleation and growth rates. These remain poorly constrained.

There are essentially two kinds of nucleation. Heterogeneous nucleation is such that the formation of nuclei of critical size is catalyzed by a solid surface in contact with the liquid (impurities). Homogeneous nucleation is such that a crystal forms without aid of foreign material, when a cluster of atoms fortuitously reaches a critical size. The rates for both phenomena can be expressed as a function of undercooling and temperature (Johnson and Mehl 1939; Turnbull and Fisher 1949). In magmas, it is not clear which

Offprint requests to: G. Brandeis

kind of nucleation dominates. Heterogeneous nucleation is probably important at small undercoolings, when the probability of formation of atom clusters is small (Chalmers 1977, pp 62–90). Crystal growth requires that chemical components be transported to the crystal surface, which is usually achieved by diffusion, and oriented into the crystal lattice (attachment). As crystallization proceeds, diffusion probably becomes limiting, determining the crystal growth rate. No method is available to treat diffusion with many interfering crystals. Thus, there is no obvious way to specify theoretically the nucleation and growth functions. One must ultimately rely on empirical expressions obtained from laboratory data and it is important to assess the precision required for realistic models and to understand the sensivity of the crystallization behaviour to the kinetic functions. This is the purpose of the present study.

The plan is the following. We study the simplest problem of conduction cooling and we carry out a dimensional analysis of the governing equations. We then give dimensionless relationships for all the crystallization parameters. In a third section, we focus on the nucleation process and show that it controls the crystallization behaviour. We then discuss the different assumptions. We finally use our results and available petrological constraints to derive bounds on the in-situ value of the nucleation rate in the interior of a large basaltic intrusion.

II Basic equations and dimensional analysis

We consider a cooling experiment in one dimension only (perpendicular to the margin). Heat transport is by conduction only. This approximation is valid in boundary layers close to the intrusion walls and will be discussed. At time $t=0$, magma is emplaced in cold country rocks. The heat equation is written:

$$\partial T/\partial t=\kappa\cdot\partial^2 T/\partial z^2 \quad \text{for } z<0 \text{ (country rock)} \tag{1a}$$

$$\partial T/\partial t=\kappa\cdot\partial^2 T/\partial z^2+L/c_p\cdot\partial\Phi/\partial t \quad \text{for } z>0 \text{ (magma)} \tag{1b}$$

where c_p is the isobaric heat capacity and L the latent heat per unit mass. Φ is the crystal content per unit volume and takes values between 0 and 1. $\partial\Phi/\partial t$ depends on the rates of nucleation and growth rates according to the equation (Kirkpatrick 1976)

$$\partial\Phi/\partial t=4\pi\cdot[1-\Phi(z,t)]\cdot Y(t)\cdot\int_0^t I(v)\cdot\left[\int_v^t Y(u)\,du\right]^2\cdot dv \tag{2}$$

where I and Y are the nucleation and growth rate functions respectively. In this equation, it is assumed that crystals are spherical and that both the nucleation and growth rates can be uniquely prescribed as a function of time at any depth z. In this paper, both rates are prescribed as a function of undercooling which in turn depends on time. In effect, this assumes that the attachment kinetics are the controlling mechanism for crystal growth, and will be discussed. To define the nucleation and growth functions, two steps are required. One is to specify a characteristic value, or scale, which introduces the nucleation and growth scales I_m and Y_m. The other step is to specify the form of the function. Standard kinetic theory leads to bell-shaped curves for both the nucleation and growth rates as a function of undercooling (Kirkpatrick 1976), called "shape 1" functions (Appendix). To investigate the influence of the form of the kinetic functions, we shall also use box-car functions, called "shape 2".

The initial conditions are that both magma and country rock are isothermal, with a temperature contrast ΔT:

$$T(z,0)=T_i \quad \text{for } z>0 \text{ (magma)} \tag{3a}$$

$$T(z,0)=T_i-\Delta T \quad \text{for } z<0 \text{ (country rocks)} \tag{3b}$$

The boundary conditions are:

$$T(+\infty,t)=T_i \tag{3c}$$

$$T(-\infty,t)=T_i-\Delta T \tag{3d}$$

T_i is the initial magma temperature, set equal to the liquidus T_L. Boundary condition (3c) states that the magma temperature is fixed far away from the margin.

The equations for T and Φ are coupled, which shows that the temperature evolution depends on the crystallization kinetics. We assume that the physical properties (κ, c_p) are constant. The temperature scale is ΔT, and the scales for the nucleation and growth rates are I_m and Y_m respectively. The time-scale appears when equation (2) is made dimensionless:

$$\tau_c=\{Y_m^3\cdot I_m\}^{-1/4} \tag{4a}$$

Heat transfer is by conduction and the length-scale is given by:

$$d_c=(\kappa\cdot\tau_c)^{1/2} \tag{4b}$$

To summarize, the knowledge of characteristic scales for the rates of nucleation and growth allow the definition of both a time-scale and length-scale. We show below that they also yield a size-scale R_c which is used to parameterize the crystal size evolution:

$$R_c=(Y_m/I_m)^{1/4} \tag{4c}$$

Non-dimensional variables are denoted by primes:

$$t=t'\cdot\tau_c \tag{5a}$$

$$z=z'\cdot d_c \tag{5b}$$

$$I=I'\cdot I_m \tag{5c}$$

$$Y=Y'\cdot Y_m \tag{5d}$$

$$T=T_i+T'\cdot\Delta T \tag{5e}$$

Equations then (1–2) become, dropping the primes:

$$\partial T/\partial t=\partial^2 T/\partial z^2 \tag{6a}$$

$$\partial T/\partial t=\partial^2 T/\partial z^2+L/(c_p\,\Delta T)\cdot\partial\Phi/\partial t \tag{6b}$$

$$\partial\Phi/\partial t=4\pi\cdot[1-\Phi(z,t)]\cdot Y(t)\cdot\int_0^t I(v)\cdot\left[\int_v^t Y(u)\,du\right]^2\cdot dv \tag{6c}$$

This introduces a non-dimensional number σ, called the Stefan number:

$$\sigma=\frac{L}{c_p\cdot\Delta T} \tag{7a}$$

Another non-dimensional number is related to the nucleation delay:

$$D=\frac{\delta T}{\Delta T} \tag{7b}$$

Table 1. List of numerical experiments

No.	L cal/g	ΔT C	I_m $cm^{-3}\,s^{-1}$	Y_m $cm \cdot s^{-1}$	I shape	Y shape	set of exp.	δT °C	τ_c s	R_c cm
2.00	86	600	$7\cdot$	$6\cdot10^{-7}$	1	1	A	$\simeq 4$	3×10^{4}	2×10^{-2}
2.01	86	600	$7\cdot$	$6\cdot10^{-5}$	1	1	A	$\simeq 4$	9×10^{2}	5×10^{-2}
2.02	86	600	$7\cdot10^{-2}$	$6\cdot10^{-6}$	1	1	A	$\simeq 4$	2×10^{4}	10^{-1}
2.03	86	600	$7\cdot10^{2}$	$6\cdot10^{-6}$	1	1	A	$\simeq 4$	2×10^{3}	10^{-2}
2.04	86	600	$7\cdot$	$6\cdot10^{-6}$	1	1	A	$\simeq 4$	5×10^{3}	3×10^{-2}
2.05	86	200	$7\cdot$	$6\cdot10^{-6}$	1	1	B	$\simeq 4$	5×10^{3}	3×10^{-2}
2.06	86	400	$7\cdot$	$6\cdot10^{-6}$	1	1	B	$\simeq 4$	5×10^{3}	3×10^{-2}
2.07	0	600	$7\cdot$	$6\cdot10^{-6}$	1	1	B–C	$\simeq 4$	5×10^{3}	3×10^{-2}
2.08	0	600	$1\cdot$	10^{-6}	2	2	C	5	3×10^{4}	3×10^{-2}
2.09	86	600	$1\cdot$	10^{-6}	2	2	C	5	3×10^{4}	3×10^{-2}
2.10	86	200	$7\cdot$	$6\cdot10^{-5}$	1	1	B	$\simeq 4$	9×10^{2}	5×10^{-2}
2.11	0	600	$7\cdot$	$6\cdot10^{-5}$	1	1	B–C	$\simeq 4$	9×10^{2}	5×10^{-2}
2.12	0	600	$1\cdot$	10^{-5}	2	2	C	5	6×10^{3}	6×10^{-2}
2.13	86	600	$7\cdot$	10^{-5}	1	2	C	$\simeq 4$	3×10^{3}	3×10^{-2}
2.15	0	600	$7\cdot$	$6\cdot10^{-4}$	1	1	B–C	$\simeq 4$	2×10^{2}	10^{-1}
2.16	0	600	$7\cdot$	$6\cdot10^{-4}$	1	2	C	$\simeq 4$	2×10^{2}	10^{-1}
2.17	86	200	$7\cdot$	$6\cdot10^{-4}$	1	1	B	$\simeq 4$	2×10^{2}	10^{-1}
2.18	86	600	$7\cdot$	$6\cdot10^{-4}$	1	1	A	$\simeq 4$	2×10^{2}	10^{-1}
2.19	0	200	$7\cdot$	$6\cdot10^{-4}$	1	1	B–C	$\simeq 4$	2×10^{2}	10^{-1}
2.20	0	600	$7\cdot$	$6\cdot10^{-4}$	2	1	C	5	2×10^{2}	10^{-1}
2.21	0	600	$7\cdot$	$6\cdot10^{-5}$	1	2	C	$\simeq 4$	9×10^{2}	5×10^{-2}
2.22	0	200	$7\cdot$	$6\cdot10^{-5}$	1	1	C	$\simeq 4$	9×10^{2}	5×10^{-2}
2.23	0	600	$7\cdot$	$6\cdot10^{-5}$	2	1	C	$\simeq 4$	9×10^{2}	5×10^{-2}
2.26	0	600	$7\cdot$	$6\cdot10^{-4}$	1+2	1	C	$\simeq 4$	2×10^{2}	10^{-1}

$c_p = 0.26$ cal/g°C, $\kappa = 7\cdot10^{-3}$ cm²/s

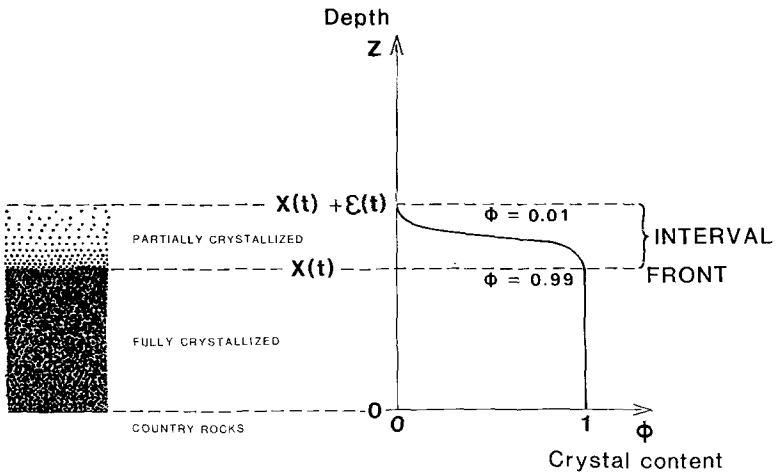

Fig. 1. Definition of the crystallization parameters. The crystallization front is the moving boundary between fully and partially crystallized magma, with coordinate $X(t)$. The region where magma is partially crystallized is called the crystallization interval. It is defined to be such that $0.01 < \phi < 0.99$ and has thickness $\varepsilon(t)$

The Stefan number gives a measure of the importance of latent heat in the temperature equation. If it is small ($\sigma \ll 1$), the effects of crystallization can be neglected in the heat budget. This does not apply to geological cases, for which the Stefan number is close to 1, thus latent heat release must be taken into account.

Because equations (6b, c) are coupled, the problem has to be solved numerically. We carry out three sets of experiments referenced in Table 1. In the first set (A), the only varying parameters are the nucleation and growth scales I_m and Y_m. In the second set (B), we investigate the role of σ. In the last set (C), we assess the influence of the shapes of the kinetic functions. Parameters κ and c_p are kept constant because they vary little for magmas, with values given in Table 1.

III The evolution of crystallization

All experiments show similar effects which have already been described in Brandeis et al. (1984). We now give dimensionless relationships for the crystallization variables. The evolution of crystallization can be followed by that of the boundary between fully and partially crystallized magma (Fig. 1). This moving boundary is called the crystallization front and is such that the crystal content Φ is equal to 0.99 (Fig. 1). Its coordinate is denoted by $X(t)$. The region where magma is partially crystallized is called the crystallization interval, defined as the zone where $0.01 < \Phi < 0.99$ (Fig. 1). Its thickness is denoted by $\varepsilon(t)$. We show below that both $X(t)$ and $\varepsilon(t)$ scale with the crystallization length-scale defined in equation (4b). Throughout the following,

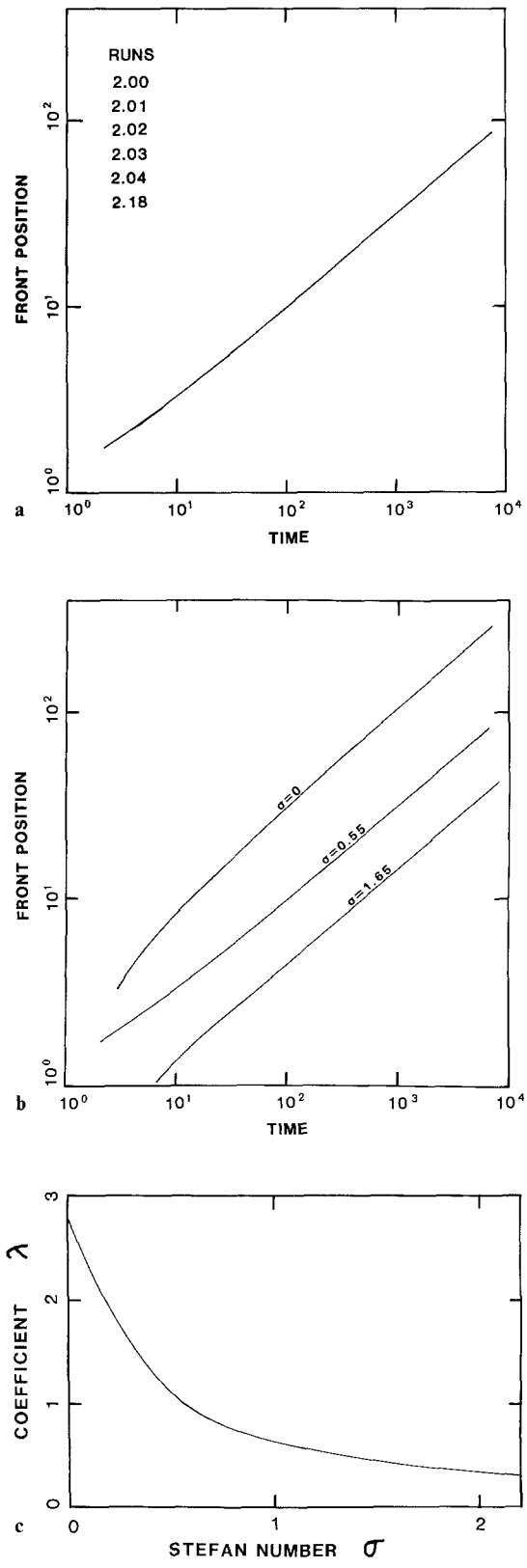

Fig. 2a, b, c. Position of the crystallization front versus time in dimensionless variables. Time $t=0$ marks the emplacement of magma in country rocks which are colder by an amount ΔT. **a** I_m and Y_m are allowed to vary. All runs (see Table 1) yield the same curve in dimensionless coordinates. This shows the validity of the dimensional analysis. **b** Curves for different values of the Stefan number σ. **c** Variation of coefficient λ in equation 9 as a function of Stefan number

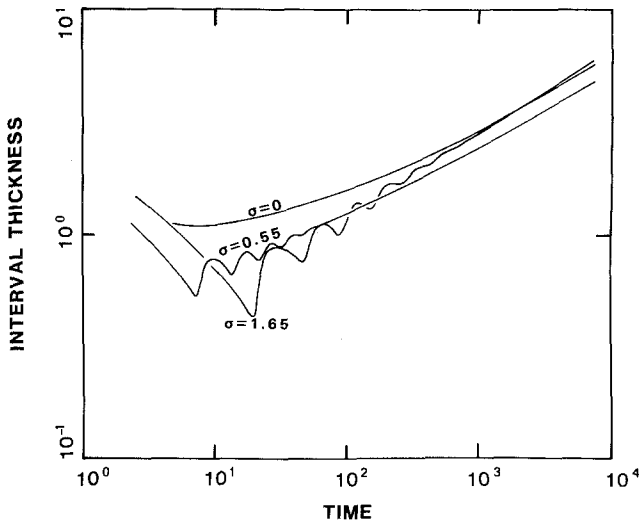

Fig. 3. Evolution of the interval thickness $\varepsilon(t)$ as a function of time in dimensionless variables for different values of the Stefan number

we make $X(t)$ and $\varepsilon(t)$ dimensionless according to the formulae:

$$X = X' \cdot d_c \tag{8a}$$

$$\varepsilon = \varepsilon' \cdot d_c \tag{8b}$$

We then drop the primes, as before.

III.1 Evolution of the crystallization interval

We first checked that all the curves of $X(t)$ are identical when I_m or Y_m are the only variable parameters (Fig. 2a). $X(t)$ follows a power-law:

$$X(t) = \lambda t^n \tag{9}$$

where exponent n is close to 1/2, but slightly different. The 1/2 power law corresponds to the ideal case of latent heat release at a fixed melting point (Jaeger 1968) or of a binary alloy without kinetic effects (Worster 1986). The crystallization kinetics do not alter significantly this simple law, due to the control by heat diffusion. Coefficient λ depends on σ, increasing with decreasing σ (Fig. 2c). This is because the smaller σ, the smaller latent heat release.

Figure 3 shows the evolution of the interval thickness $\varepsilon(t)$. The general trend is a slow increase with a few oscillations which reflect the discontinuous behaviour of crystallization in transient conditions. Brandeis et al. (1984) showed that nucleation occurs as sharp pulses followed by longer periods of crystal growth, leading to temperature fluctuations. The effect is described in more detail below.

When varying the nucleation and growth scales, we found again that all curves of $\varepsilon(t)$ are superposed, which shows the valididy of the scaling procedure. Reverting to dimensional variables, this implies that ε is inversely proportional to I_m. It appears that the variation of $\log(\varepsilon)$ as a function of $\log(t)$ is quasi-linear. In each case, the data can be fit to a few percent with a law (in dimensionless variables):

$$\varepsilon(t) = \alpha \cdot t^{\beta} \tag{10}$$

Exponent β is about to $\simeq 0.37$ for $\sigma = 1.65$ and has a limit value of 0.29 for $\sigma = 0$. Coefficient α is close to 0.3.

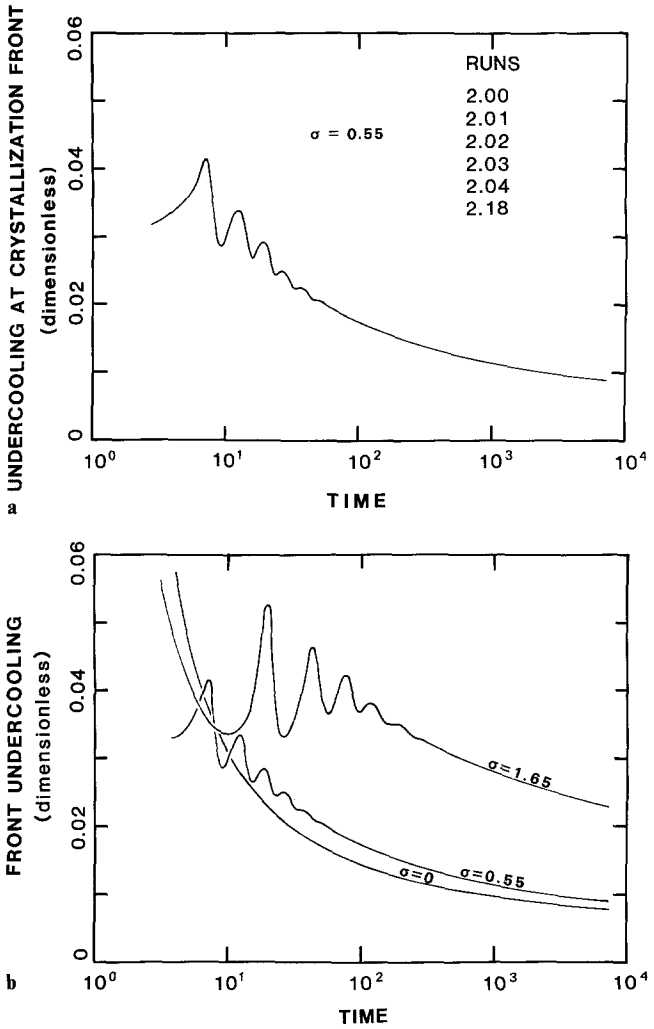

Fig. 4a, b. Dimensionless undercooling at the crystallization front $\theta(t)$ as a function of time (also dimensionless) when: **a** I_m and Y_m are the only variable parameters (set A) **b** σ is the only variable parameter (set B)

Relationships (9) and (10) are dimensionless and can be used for any values of the nucleation and growth scales. They represent universal results extending those by Brandeis et al. (1984).

III.2 Thermal evolution

To follow temperature in crystallizing magma, we use the dimensionless undercooling at the crystallization front:

$$\theta(t)=\frac{T_L-T[X(t),t]}{\Delta T} \tag{11}$$

We again verified the validity of the dimensional analysis by comparing results from different runs (Fig. 4a). θ decreases with a few oscillations due to the discontinuous character of nucleation. The oscillations are damped as there is a tendency to achieve a balance between latent heat release and heat loss. They are not of numerical origin, as shown by systematic checks on the convergence of the solutions. A simplified analysis of this problem can be found in Brandeis et al. (1984), which explains that oscillatory behaviour is the natural consequence of the coupling between latent heat release and temperature. The analysis shows further that damping depends on the steepness of the nucleation and growth curves.

In Fig. 4a, all curves are superposed. The calculations have been made with different parameters, time-steps and space-steps. The fact that all solutions fall on the same dimensionless curve emphasizes that the oscillations are real, not numerical. The physical explanation is the following. Following emplacement in cold country rocks, undercoolings are high and nuclei are formed in large numbers, releasing large amounts of latent heat. This increases the magma temperature and hence stops nucleation. Latent heat is then released at a reduced rate and cooling is allowed to proceed, promoting the formation of another batch of nuclei and hence of another temperature fluctuation.

Note that θ has not been calculated for times $t<1$ (in dimensional variables, for times smaller than the crystallization time-scale), because crystallization has not started, and hence there is no crystallization front. This shows that τ_c is close to the time for crystallization to start in supercooled magma.

Figure 4b, illustrates the influence of the Stefan number σ. The larger σ, the larger the temperature oscillations, because latent heat is conducted away with less and less efficiency. There are no oscillations for $\sigma=0$, as there is no latent heat effect. A striking fact is that the number of oscillations does not depend on σ. We interpret this as the number of characteristic times needed to achieve quasi-equilibrium conditions. In other words, it takes a given number of crystallization times to forget the initial conditions. In the simplified analysis of Brandeis et al. (1984), the crystallization behaviour depends on two parameters, one of which defines the intensity of damping and hence the number of oscillations which can be observed. The other parameter determines the intensity of oscillations and depends on the Stefan number, accounting for the effects described here.

III.3 The crystal size

We also calculate the crystal size. In dimensional variables, a unit volume of crystallized material comprises N crystals, with mean radius R:

$$N(z)=\int_0^\infty [1-\Phi(z,t)]\cdot I(t)\cdot dt \tag{12a}$$

$$R(z)=[4/3\cdot\pi\cdot N(z)]^{-1/3} \tag{12b}$$

A size-scale appears when equation (12) is made dimensionless:

$$R_c=\{Y_m/I_m\}^{1/4} \tag{13}$$

The dimensionless crystal size is obtained by:

$$R'=\frac{R}{Rc} \tag{14}$$

R varies as a function of the distance from the margin. Again, all dimensionless curves are identical proving that R_c is the correct size-scale (Fig. 5a).

Extrapolating these results to a wide range of natural cases is difficult because, far from the margins, crystallization proceeds at small undercoolings in conditions where our knowledge of the nucleation process is poor. The labo-

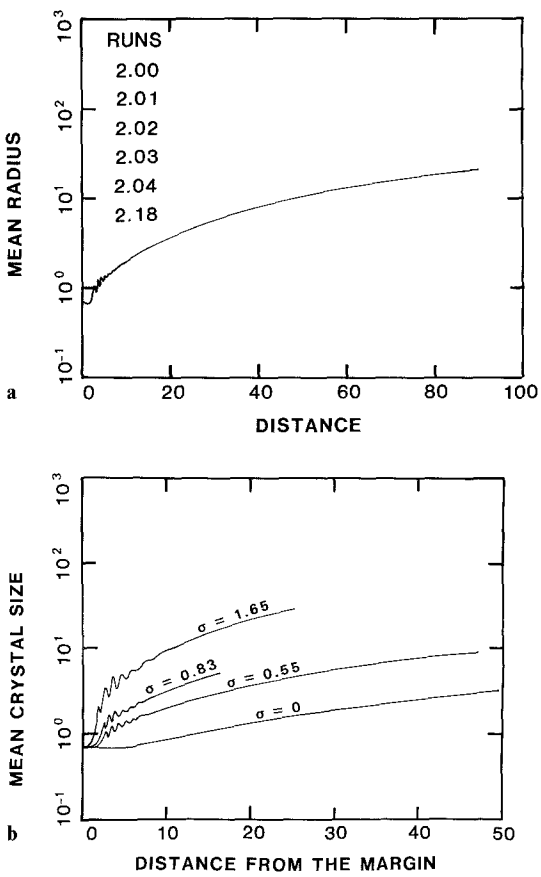

Fig. 5a, b. Mean Crystal size (radius) versus distance from the margin in dimensionless variables for different values of the Stefan number σ. **a** All results for $\sigma = 0.55$. **b** Comparison for different values of σ

ratory experiments of Fenn (1977), Swanson (1977) and Tsuchiyama (1983) bring constraints only on the peak nucleation rate. The shape 1 function used so far relies on parameters derived from standard kinetic theory (see Appendix). For such a function, the nucleation rate tends to zero continuously with decreasing undercooling. The unavoidable consequence is that the crystal size may eventually reach infinity. Specifically, what is needed is some information on the shape of the nucleation function.

IV The influence of the shape of the kinetic functions

We investigate the effects of shape 2 kinetic functions (see the Appendix), which represent the limit-case of discontinuous behaviour. For the nucleation process, this is not unreasonable and approximates the effect of a finite energy barrier for the formation of a nucleus. Intuitively, these functions represent the obvious way to achieve a constant crystal size throughout the crystallization sequence. These functions are not meant to be realistic, but to provide a test of how sensitive to the kinetic functions the crystallization behaviour.

We have made calculations for all possible combinations of shape 1 and shape 2 functions, keeping the same procedure for making variables dimensionless. σ is taken to be zero. This case is simpler, yet shows all the important features as σ has no effect on the form of the relationship between the crystallization parameters.

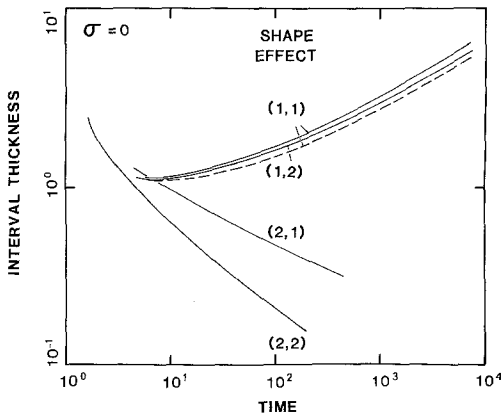

Fig. 6. Evolution of the interval thickness $\varepsilon(t)$ for different shapes of the kinetic functions (set C). The *first* and *second number in brackets* refer to the shapes of the nucleation and growth functions respectively. The Stefan number is set equal to 0. Non dimensional number D (dimensionless nucleation delay, equation 7b) takes values of 6.7×10^3 (*plain curves*) and 2×10^{-2} (*dashed curve*)

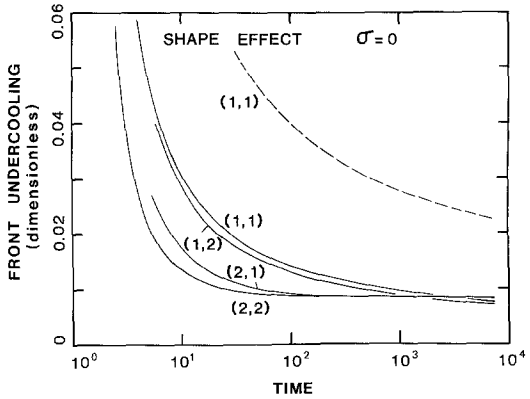

Fig. 7. Evolution of the front undercooling $\theta(t)$ for different shapes of the kinetic functions (set C). The Stefan number is equal to 0. *Plain* and *dashed curves* are as in Fig. 6

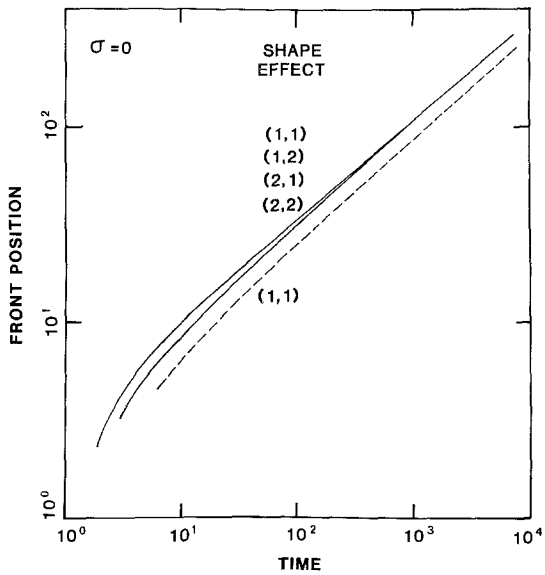

Fig. 8. Evolution of the front position $X(t)$ for different shapes of the kinetic functions (set C). The Stefan number is equal to 0. *Plain* and *dashed curves* are as in Figs. 6 and 7

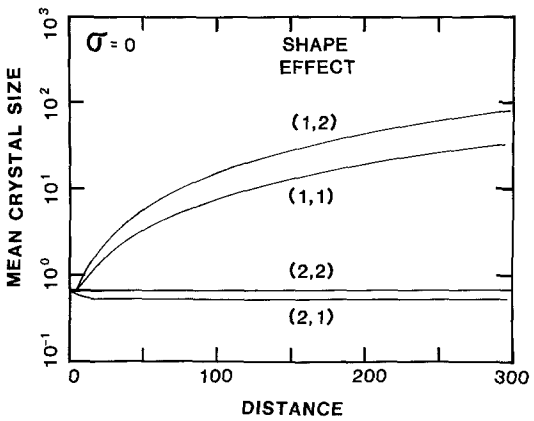

Fig. 9. Evolution of the mean crystal radius as a function of distance from the margin for different shapes of the kinetic functions (set C). The Stefan number is equal to 0

For a shape 2 nucleation function, ε decreases with time (Fig. 6), because undercoolings in the crystallization interval decrease towards limit δT (Fig. 7). The shape of the growth function has no influence on ε or θ, having only a weak effect on the numerical values. This is an important fact to which we shall return. The crystallization front position follows exactly the square-root of time (Fig. 8). This agrees exactly with Jaeger's model (1968) because of the tendency to crystallize over an interval of negligible thickness.

The effect on crystal sizes is more interesting. For a shape 2 nucleation function, the crystal size is constant after a small transient (Fig. 9). The value is close to the size-scale defined by (13), with a proportionality constant between 0.5 and 0.7 depending on the shape of the growth function.

We conclude that the shape of the nucleation function has a critical influence on the results, contrary to that of the growth function. It is nucleation which is responsible for temperature oscillations as well as the tendency to maintain a constant crystal size. Crystal growth does play a role in determining the numerical constants in the various scaling laws, but does not have any effect on the crystallization behaviour.

V Discussion

A comparison between these results and those by Jaeger (1968) can be found in Brandeis et al. (1984). To make a quantitative model for petrological applications requires numerical values for the various parameters. The nucleation and growth scales have been factored out of the equations and need only be specified in a last step. One must specify the Stefan number. In conditions of intrusion into upper crustal rocks, the initial temperature contrast ranges from about 600° C to 1000° C, depending on the liquidus temperature. Latent heat values vary between 50 and 200 cal/g. Thus, σ varies between about 0.2 and 1.3. For basaltic magmas with high temperatures, the range is smaller and a representative value is 0.4. The other non-dimensional number is D (7b). This second number is important because it determines the temperature range over which there is no nucleation. As crystallization proceeds, the dimensionless undercooling at the crystallization front tends towards D (Fig. 7). From available laboratory data, the nucleation delay δT never exceeds a few tens of degrees (Gibb 1974; Donaldson 1979), and hence is always much smaller than the initial temperature contrast. For the heat budget, number D is always small and plays little role, as shown by its weak influence on the front position and on the interval thickness (Figs. 6 and 8).

We now discuss our assumptions.

V.1 The crystallization kinetics

Crystal growth is affected by both chemical diffusion and the attachment kinetics. The rate controlling process is the slowest one. In rapidly cooled magma such as lava flows, chilled margins, or laboratory samples, spherulitic or dendritic morphologies show that diffusion is limiting. In large intrusions, monomineralic layers thicker than 10 m are commonly observed (Wager and Brown 1968), indicating that the chemical evolution of crystallizing magma is not obvious. For example, compositional convection may occur in the porous cumulate pile (Morse 1969; Tait et al. 1984; Kerr and Tait 1986), bringing the required components to achieve adcumulate growth. We have shown that the shape of the growth function has no influence on the results. Therefore, only the magnitude of the growth rate is important. One needs only select an overall value consistent with the rate of solute transport (by diffusion or else).

Turning to the nucleation function, the most important result of this study is that its shape is a critical factor, especially at small undercoolings. In particular, it is reflected directly in the crystal size variation (Fig. 9). A key observation is that the crystal size varies little in the interior of large igneous complexes. A shape 1 nucleation function implies large size variations, which does not seem compatible with observations. Further, crystal sizes from intrusions of all types, sizes and shapes are remarkably similar (Brandeis et al. 1984), even though cooling conditions must have been quite different. This suggests that the nucleation function does not vary rapidly when undercoolings are small, and hence, to be specific, differs from a shape 1 function. This raises the difficult problem of determining precisely the nucleation function close to the liquidus. For natural silicate compositions, nucleation rates in those conditions are very small implying extremely long crystallization times (see below), and hence making laboratory experiments difficult. The uniformity of crystal sizes suggests that the nucleation rate varies little in the interior of large intrusions. The limit-case is that of a constant, i.e., a shape 2 function, which is the best approximation at the moment.

We conclude that, to explain both crystal size variations at the margins as well as their lack of variation in the interior, the simplest nucleation function is a combination of shape 1 and shape 2 functions. We show in Fig. 10 such a function, used in a final calculation. The corresponding crystal size curve is given in Fig. 11 and shows both features: a sharp increase at the contact, followed by convergence towards a limit value. In this example, one must carry out two separate scaling analyses. One for highly transient conditions pertaining to the margin, where shape 1 functions must be used. The other for quasi-equilibrium conditions prevailing in the interior, where a shape 2 nucleation function must be used.

V.2 Thermal regime

We have considered cooling by conduction only, which is valid in thin dikes and sills, but also at the bottom of intru-

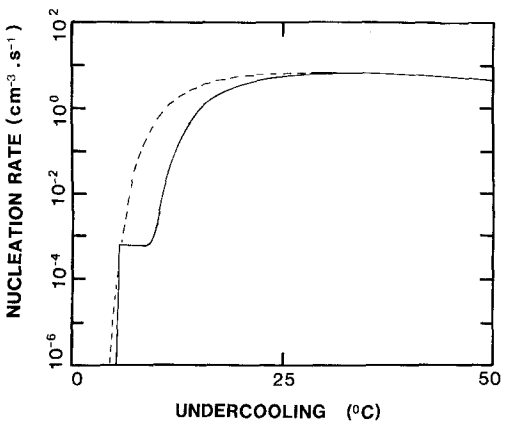

Fig. 10. Combination of shape 1 and shape 2 nucleation functions (*plain curve*). The shape 1 function is shown for comparison (*dashed curve*)

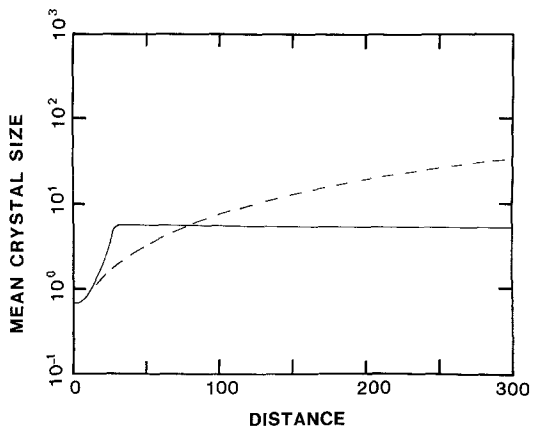

Fig. 11. Dimensionless crystal size as a function of distance from the margin for the nucleation function of Fig. 10 (*plain curve*). The *dashed curve* shows the result for a shape 1 nucleation function. Both calculations are made with a shape 1 growth function

sions. There, crystallization occurs mainly in situ (Campbell 1978; McBirney and Noyes 1979) in stagnant layers isolated from convection (Jackson 1961; Jaupart and Brandeis 1986).

A more important limitation is boundary condition (3c), where the magma temperature far from the margin is held constant. In reality, the intrusion must cool and its interior temperature must decrease. This invalidates the boundary condition which must be replaced by some function of time. However, the intrusion cooling occurs over a rather large time, for both conduction and convection (see, for example, Jaupart and Brandeis 1986), and hence the solutions derived above are valid over a large time and hence distance. It is not our purpose to dwell longer on the complex thermal evolution of magma chambers, which is not fully understood yet, but the general consequence is easy to predict: undercooling in the crystallization interval will be somewhat larger than in our calculations, and hence the crystal size will be somewhat smaller. For example, dikes with decreasing widths cool with increasing efficiency and should exhibit decreasing crystal sizes, which is indeed observed (Ikeda 1977).

For large magma chambers, given the complexity of their thermal regime, it seems impossible to use the preceding analysis. Adding the difficulty of determining nucleation rates at small undercoolings, perspectives appear quite uncertain. However, we now show that our results can be plausibly extended to a variety of more complex cases. Consider the evolution of the crystallization parameters: for example, the crystal size increase away from the margin, or the increase of the interval thickness with time. They reflect the evolution of undercoolings in the crystallization interval illustrated in Fig. 4.: as time increases, undercoolings decrease. Thus, the nucleation and growth rates also decrease, implying the increase of crystal size and interval thickness which is found. More precisely, it is possible to use local scaling laws based on the mean undercooling θ^* which prevails at the time each piece of magma crystallizes. From those, we define the local scales:

$$R^* = [Y(\theta^*)/I(\theta^*)]^{1/4} \tag{15a}$$

$$\tau^* = [I(\theta^*) \cdot Y(\theta^*)^3]^{-1/4} \tag{15b}$$

$$d^* = \sqrt{\kappa \tau^*} \tag{15c}$$

Using the value θ^* from Fig. 4 in those relations yields the observed curves for the crystal size, the interval thickness, etc.... This is powerful because only the local values of the nucleation and growth rates are required, regardless of the whole kinetic functions. For example, following emplacement in cold rocks, undercoolings are the highest, and magma crystallizes at the peak rates. Indeed, we found that the dimensionless crystal size close to the margin was close to 1, which, in dimensional variables, means that the crystal size is given by equation (15a) using the peak rates. Obviously, the local scaling procedure is also valid for shape 2 functions.

We emphasize that the procedure holds in the very transient conditions of our sudden cooling experiment. Even in those conditions, a piece of magma crystallizes fast enough so that it does not experience highly variable undercoolings. However, from one piece of magma to the neighbouring one, thermal conditions are slightly different, leading to the systematic variation of crystallization parameters which is observed. The fact that the local scaling laws are successful in those transient conditions suggest that they can be applied to other cases as well, where the intrusion cools by processes other than conduction. Certainly, the crystallization time-scale can be found from the crystal content equation (2) without any assumption on the thermal regime. The same is true for the crystal size-scale. The thickness of the crystallization interval is more sensitive, because it is directly related to the temperature gradient and hence to the heat transport mechanism (see Brandeis et al. 1984).

The local scaling laws are very powerful because the crystal size can be measured and provides a direct constraint on the local nucleation and growth rates. A single additional constraint is therefore sufficient to determine both rates. This is attempted in the next section.

VI Constraints on the kinetic rates from observations

Two separate analyses can be made. One for the vicinity of margins where shape 1 functions can be used. The other with shape 2 functions for quasi-equilibrium condition in the interior.

VI.1 The margins

A few crystal size data are available for dikes and sills (summarized in Walker et al. 1976). We use measurements from

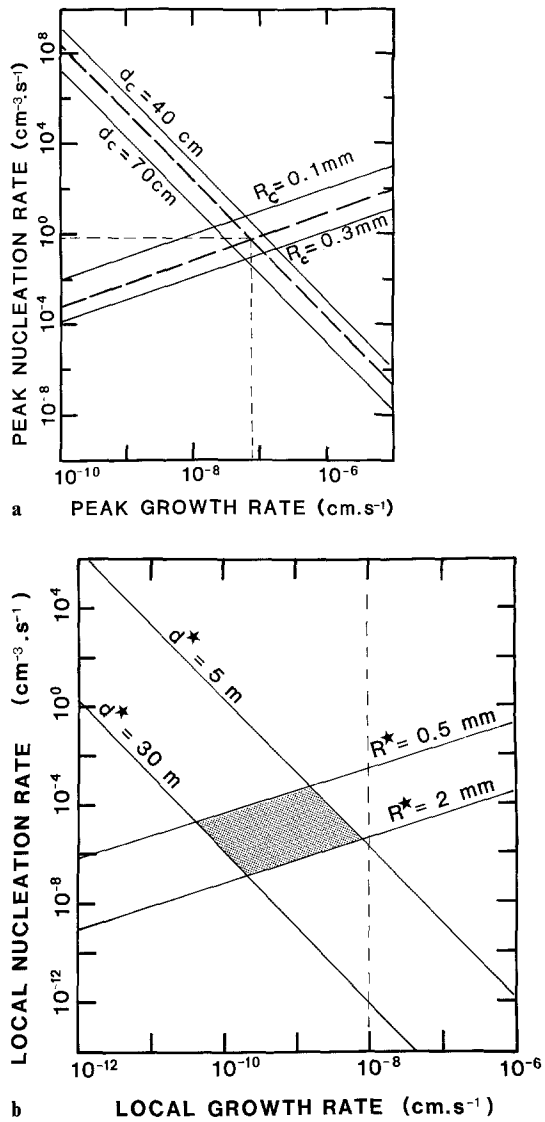

Fig. 12a, b. Relationships between the values of the nucleation and growth rates: **a** in transient conditions prevailing close to margins **b** in quasi-equilibrium conditions prevailing in the interior of large magma chambers. The curves are defined by equations (17a) and (17b) (case **a**), or (18a) and (18b) (case **b**). Their intersection define the domain of plausible values for the kinetic rates in natural conditions

basic dikes (Gray 1970; Walker 1940) which show similar curves of crystal size as a function of distance to the margin. We use shape 1 functions, with the nucleation and growth scales denoted by I_1 and Y_1 respectively.

The crystal size curve can be quite complex very close to the margin, with sometimes a chill zone forming (Brandeis et al. 1984). Walker et al. (1976) proposed a relationship between crystal size R and the distance from the margin X of the form:

$$R = k_1 X^n \tag{16}$$

where n is usually between 0.3 and 0.6. As shown by Fig. 5, our results look similar to such a power-law relationship. For Stefan numbers smaller than 0.5, which should be the case of basic magmas (see above), we find that exponent n is about 0.8 far from the margin. Very close to the margin, results depart from a power-law. Forcing a power-law relationship from the very margin inwards yields much lower values of n, similar to those proposed by Walker et al. (1976), but without a firm basis.

The universal curves of Fig. 5 can be fit to the data of Walker (1940) and Gray (1970) by adjusting the size-scale and length-scale. As shown by Fig. 5b, the crystal size in the vicinity of the margin is very close to the size-scale. Thus, the measured value gives directly ratio (Y_1/I_1), which yields a relationship between the nucleation and the growth rate:

$$I_1 = Y_1/R_c^4 \tag{17a}$$

Away from the margins, the crystal size exhibits a ten-fold increase over a typical distance of 5 m, with lower and upper bounds of 4 and 7 m (Winkler 1949; Gray 1970; Walker 1940). In our calculations, this increase occurs over a dimensionless distance of about 10, i.e., over ten times the crystallization length-scale (Figs. 5 and 9). Thus, this length-scale (defined by equation 4b) is between 40 and 70 cm. Using a thermal diffusivity of 10^{-6} m^2/s, this yields a second relation between the nucleation and growth scales:

$$I_1 = Y_1^{-3} \cdot \tau_c^{-4} \tag{17b}$$

The intersections of the two curves define a domain of plausible values. Estimates of 10^{-7} cm/s and 1 cm^{-3} s^{-1} are found for the growth and nucleation scales respectively, corresponding to a crystallization time scale of 2×10^5 s. The range of growth scales spans only one order of magnitude, whereas that for the nucleation scale spans about two orders of magnitude (Fig. 12a). This growth scale is close to the values of Swanson (1977) and Swanson and Fenn (1986). The nucleation scale is compatible with the bounds of 10^{-2} and 10^2 cm^{-3} s^{-1} obtained from laboratory experiments (Brandeis et al. 1984; Tsuchiyama 1983).

VI.2 The interior of magma chambers

Consider now quasi-equilibrium conditions at small undercoolings. We use shape 2 functions with scales I_2 and Y_2. The crystal size yields again a relationship:

$$I_2 \simeq Y_2/R^{*4} \tag{18a}$$

The typical crystal size is 1 mm in basic intrusions and can vary between 0.5 and 2 mm. We report on Fig. 12b I_2 as a function of Y_2 according to this equation.

It is possible to derive a second constraint from the local thickness of the crystallization interval ε^* which scales with the local length-scale d^* (equation 15c). It cannot be measured directly for obvious reasons, but petrological observations can be used for constraints. One concerns the lack of evidence for crystal settling. If the thickness of the crystallization interval was large, crystal settling would be significant and lead to visible sorting. Indeed, evidence for sorting exists in a small number of cases over vertical distances less than 1 m (Irvine 1974; Brown and Farmer 1971). Another observation is the thickness of the crystal mush which is disturbed by magma currents. This mush is the pile of loosely consolidated crystals which lies at the chamber bottom. In our definition, it is simply the crystallization interval. Several authors have inferred that its thickness is a few metres (Hess 1960; Parsons and Butterfield 1981).

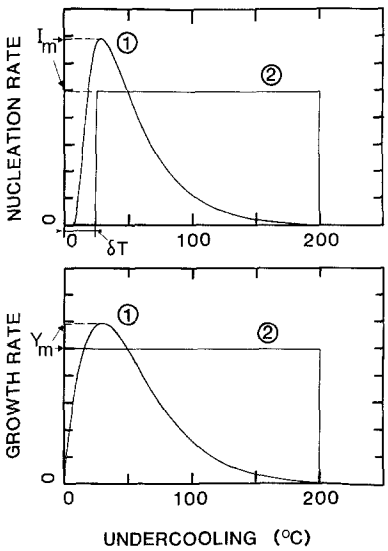

Fig. 13. The functions used for the nucleation and growth rates as a function of undercooling. Shape 1 functions correspond to standard kinetic theory. Shape 2 functions are used to investigate the role played by the shape of the kinetic functions. For numerical applications, the nucleation and growth scales I_m and Y_m must be specified. Note the difference between the nucleation and growth functions close to the liquidus (zero undercooling): there is a nucleation delay δT

For the sake of discussion, we consider that the thickness of the crystallization interval can vary between 50 cm and 3 m. We therefore write the conditions:

$$I_2 = Y_2^{-3} \cdot \tau^{*-4} \tag{18b}$$

and:

$$\frac{d^*}{\varepsilon^*} = \alpha \tag{18c}$$

where α is a coefficient varying between 1 and 10 depending on the shape of the nucleation function (Fig. 6). Assuming again a thermal diffusivity of 10^{-6} m^2/s, we report on Fig. 12b the corresponding relationship between the nucleation and growth rates. Again, this defines a domain of plausible values. The uncertainties given by relation (18b) are greater than in the previous case, because of the large range of values for ε^* and therefore d^*.

We find that the growth rate must be between 10^{-10} and 10^{-8} cm/s, and the nucleation rate between 10^{-7} and 10^{-3} cm^{-3} s^{-1} (Fig. 12b). This yields a range of crystallization times of $10^7 - 10^9$ s. Note that, although the ranges of kinetic rates are large, they allow rather tight constraints on the crystallization parameters of interest: time-scale and length-scale. This is due to their weak dependence on the kinetic rates.

These values can be compared to data obtained in natural cooling conditions in Hawaiian basaltic lava lakes. In these, the thermal evolution is complex, with hydrothermal convection in the fractured crust and differs from that assumed in this study. However, the measured values correspond to some undercooling and must thus be bounded by the values I_1 and I_2 for nucleation and Y_1 and Y_2 for growth. Kirkpatrick (1977) estimated growth rates between 10^{-10} and 10^{-9} cm·s^{-1} for plagioclase crystals, and nucleation rates between $7 \cdot 10^{-3}$ and 2 cm^{-3}·s^{-1}. These are consistant with our estimates.

VII Conclusion

We have shown how the kinetics of nucleation and crystal growth determine the crystallization behavior. Scaling laws have been derived which allow simple definitions of the main crystallization parameters. For crystallization, the most important process is nucleation, which is unfortunately not very well known at small undercoolings. We show that crystal size data yield simple constraints relating the nucleation and growth rates. Using petrological observations, we have obtained bounds at 10^{-7} and 10^{-3} cm^{-3} s^{-1} for the nucleation rate which prevail in the deep interior of basaltic magma chambers. The range is large and therefore seems of little practical interest. However, it allows useful constraints on the crystallization parameters of interest. For example, the crystallization time-scale must be between 10^7 and 10^9 s.

Appendix

A.I The kinetics of crystallization

A.I.1 The nucleation rate. The critical parameter is the temperature interval δT, called the nucleation delay, over which the nucleation rate is negligible (Dowty 1980). The δT does not exceed a few tens of degrees for magmas (Gibb 1974; Donaldson 1979). Using parameters suitable for heteregeneous nucleation we obtain, an expression following Turnbull and Fisher (1949) and Turnbull (1950, 1952):

$$I_1 = K_1 \cdot T \cdot \exp[-K_2/(T\psi^2)] \cdot \exp(-K_3/T) \tag{A1}$$

where T is the absolute temperature and ψ the undercooling $T_L - T \cdot K_1$, K_2 and K_3 determine respectively the peak nucleation rate, the nucleation delay δT and the temperature interval over which nucleation occurs. In this paper, K_1 is allowed to vary while K_2 and K_3 are kept constant. I_1 is thus a function of the single variable undercooling ψ and its shape, referenced as shape 1, is fixed (Fig. 13).

To investigate the influence of the shape of the function, we use a box-car function called shape 2: I_2 is zero for $\psi < \delta T$ and $\psi > 200°$ C, and has a constant value between these two temperatures (Fig. 13).

A.I.2 The growth rate. In highly transient cooling conditions, crystal growth is controlled by the interface reactions with a growth rate depending on undercooling (Kirkpatrick 1975; Baronnet 1984). Chemical diffusion eventually becomes limiting on a small-scale (Lasaga 1982; Loomis 1982). For attachment-controlled growth, we take the simplest law as a function of temperature, following Kirkpatrick (1975):

$$Y_1 = K_4 \cdot [1 - \exp(-K_5\psi/T)] \cdot \exp(-K_6/T) \tag{A2}$$

In this paper, K_4 is allowed to vary while K_5 and K_6 are kept constant. This is the shape 1 function.

We also consider a box-car function called shape 2: Y is constant over the undercooling interval [0.200° C] and zero elsewhere. The two functions are represented on Fig. 13.

A.I.3 Numerical values. For shape 1 functions, the values of parameters K_2, K_3 and K_5, K_6 are obtained with available data on silicate melts (for more details, see Dowty (1980)). We have taken $K_2 = 5 \times 10^5\ K^{-3}$, $K_3 = K_6 = 6 \times 10^4 K$, and $K_5 = 20$. The nucleation delay is equal to $\simeq 4°$ C, close to measured values in basaltic

melts (Donaldson 1979). For those functions, the scales are given by the peak values. For "shape 2" functions, the scale is simply the constant value taken by the function.

References

Baker MB, Grove TL (1985) Kinetic controls on pyroxene nucleation and metastable liquid lines of descent in a basaltic andesite. Am Mineral 70:279–287

Baronnet A (1984) Growth kinetics of the silicates. A review of basic concepts, Fortschr Mineral 62:187–232

Brandeis G, Jaupart C, Allegre CJ (1984) Nucleation, crystal growth and the thermal regime of cooling magmas. J Geophys Res 89:10161–10177

Brown PE, Farmer DG (1971) Size-graded layering in the Imilik gabbro, East Greenland. Geol Mag 108:465–476

Campbell IH (1978) Some problems with the cumulus theory. Lithos 11:311–323

Chalmers B (1977) Principles of solidification Florida, Krieger Publishing Company

Donaldson CH (1979) An experimental investigation of the delay in nucleation of olivine in mafic magmas. Contrib Mineral Petrol 69:21–32

Dowty E (1980) Crystal growth and nucleation theory and the numerical simulation of igneous crystallization. In: Hargraves RB (ed) Physics of magmatic processes, Princeton, University Press, pp 419–485

Fenn PM (1977) The nucleation and growth of alkali feldspars from hydrous melts. Can Mineral 15:135–161

Gibb FGF (1974) Supercooling and crystallization of plagioclase from a basaltic magma. Mineral Mag 39:641–653

Gray NH (1970) Crystal growth and nucleation in two large diabase dikes. Can J Earth Sci 7:366–375

Hess HH (1960) Stillwater igneous complex. Geol Soc Am Mem 80:230

Ikeda Y (1977) Grain size of plagioclase of the basaltic andesite dikes, Iritono, Central Abukuma Plateau. Can J Earth Sci 14:1860–1866

Irvine TN (1974) Petrology of the Duke Island ultramafic complex, Southeastern Alaska. Geol Soc Am Mem, p 138

Jaeger JC (1968) Cooling and solidification of igneous rocks. In: Hess HH, Poldervaart A (eds) Basalts: The Poldervaart treatise on rocks of basaltic composition, vol 2, New York, John Wiley & Sons Inc, New York, pp 503–536

Jackson ED (1961) Primary textures and mineral associations in the ultramafic zone of the Stillwater complex, Montana. Geol Surv Prof Pap 358:106

Jaupart C, Brandeis G (1986) The stagnant bottom layer of convecting magma chambers. Earth Planet Sci Lett 80:183–199

Johnson WA, Mehl RF (1939) Reaction kinetics in processes of nucleation and growth. Trans AIME 135:416–442

Kerr RC, Tait SR (1986) Crystallization and compositional convection in a porous medium with application to layered intrusions. J Geophys Res 91:3591–3608

Kirkpatrick RJ (1975) Crystal growth from the melt: a review. Am Mineral 60:798–814

Kirkpatrick RJ (1976) Towards a kinetic model for the crystallization of magma bodies. J Geophys Res 81:2565–2571

Kirkpatrick RJ (1977) Nucleation and growth of plagioclase, Makaopuhi and Alae lava lakes, Kilauea Volcano, Hawaii. Geol Soc Am Bull 88:78–84

Kirkpatrick RJ, Kuo LC, Melchior J (1983) Crystal growth in incongruently melting compositions: programmed cooling experiments with diopside. Am Mineral 66:223–241

Lasaga AC (1982) Towards a master equation in crystal growth. Am J Sci 282:1264–1320

Lofgren GE (1980) Experimental studies on the dynamic crystallization of silicate melts. In: Hargraves RB (ed) Physics of magmatic processes. Princeton Univ Press, Princeton, pp 487–551

Loomis TP (1982) Numerical simulations of crystallization processes of plagioclase in complex melts: the origin of major and oscillatory zoning in plagioclase. Contrib Mineral Petrol 81:219–229

McBirney AR, Noyes RM (1979) Crystallization and layering of the Skaergaard intrusion. J Petrol 20:487–554

Morse SA (1969) The Kiglapait layered intrusion, Labrador. Geol Soc Am Mem, p 112

Parsons I, Butterfield AW (1981) Sedimentary features of the Nunarssuit and Klokken syenites, S. Greenland. J Geol Soc London 138:289–306

Swanson SE (1977) Relation of nucleation and crystal-growth rate to the development of granitic textures. Am Mineral 62:966–978

Swanson SE, Fenn PM (1986) Quartz crystallization in igneous rocks. Am Mineral 71:331–342

Tait SR, Huppert HE, Sparks RSJ (1984) The role of compositional convection in the formation of adcumulate rocks. Lithos 17:139–146

Turnbull D (1950) Formation of crystal nuclei in liquid metals. J Appl Phys 21:1022–1028

Turnbull D (1952) Kinetics of solidification of supercooled liquid mercury droplets. J Chem Phys 20:411–424

Turnbull D, Fisher JC (1949) Rate of nucleation in condensed systems. J Chem Phys 17:71–73

Tsuchiyama A (1983) Crystallization kinetics in the system $CaMgSi_2O_6-CaAl_2Si_2O_8$: the delay in nucleation of diopside and anorthite. Am Mineral 68:687–698

Wager LR, Brown GM (1968) Layered Igneous rocks. Oliver and Boyd, Edinburgh, p 588

Walker F (1940) Differentiation of the Palisade diabase, New Jersey. Bull Geol Soc Am 51:1059–1106

Walker D, Longhi J, Kirkpatrick RJ, Hays JF (1976) Differenciation of on Apollo 12 picrite magma. Proc Lunar Sci Conf 7th, pp 1365–1389

Winkler HGF (1949) Crystallization of basaltic magma as recorded by variation of crystal size in dikes. Mineral Mag 28:557–574

Worster MG (1986) Solidification of an alloy from a cooled boundary. J Fluid Mech 167:481–501

Received August 4, 1986/Accepted January 26, 1987